

# Bond behaviour of smooth surface GFRP pultruded profiles with cement grout

Mamun Abdullah, Wahid Ferdous<sup>\*</sup>, Sourish Banerjee, Allan Manalo

University of Southern Queensland, Centre for Future Materials (CFM), School of Engineering, QLD 4350, Australia

## ARTICLE INFO

### Keywords:

Bond behaviour  
GFRP  
Cement grout  
Glass sand  
Analytical model

## ABSTRACT

The advantages of glass fibre reinforced polymer (GFRP) pultruded composite profiles, such as their high strength-to-weight ratio, corrosion resistance, and low maintenance costs, have attracted the attention of researchers and end users in structural applications. In spite of this, one of the challenges associated with using GFRP pultruded profiles is their smooth surfaces when bonded with concrete. To address this challenge, this study investigated four different approaches that can be used to improve the bond performance between GFRP pultruded profiles and concrete surfaces. These approaches are the incorporation of glass sand into cement grout, the variation in the size of the sand particles in the grout, the surface preparation of GFRP profiles, and the use of various cement characteristics. The experimental results show that the surface preparation of the GFRP profiles is the most effective method of improving the bond strength between the GFRP profiles and the concrete surface. Additionally, a theoretical model is developed to predict the bond behaviour, and it is observed that the linear elastic theory with the inclusion of the bond surface roughness coefficient is capable of predicting bond behaviour. The overall outcome of the study will assist design engineers and end users in the application of smooth surface GFRP profiles in concrete structures.

## 1. Introduction

In recent years, pultruded GFRP profiles have grown in popularity due to the increasing demand for lightweight, durable, corrosion-resistant materials across a variety of industries as well as advancements in manufacturing techniques and material formulations [1–3]. GFRP pultruded composite profiles are widely applied in civil engineering for infrastructure enhancement, performing an important role in retrofitting and strengthening existing structures such as bridges, buildings, and historical structures [4–10]. In order to meet the evolving demands for sustainable and resilient urban development, they can be designed in a variety of ways with a range of flexibility.

Pultruded GFRP profiles have been considered as an application for the development of composite railway sleepers. A study was conducted by Ferdous et al. [11] involving pultruded hollow GFRP profiles filled with rubberised cement concrete, and the beams were embedded in softer polymer concrete in order to manufacture composite railway sleepers. It was found that the railway sleeper concept was able to create a good bond between polymer concrete and GFRP profiles in this study. However, resin-based polymer concrete is a

<sup>\*</sup> Correspondence to: University of Southern Queensland, Centre for Future Materials (CFM), School of Engineering, Toowoomba, QLD 4350, Australia.

E-mail addresses: [Mamun.AlMamun@unisq.edu.au](mailto:Mamun.AlMamun@unisq.edu.au) (M. Abdullah), [Wahid.Ferdous@unisq.edu.au](mailto:Wahid.Ferdous@unisq.edu.au) (W. Ferdous), [Sourish.Banerjee@unisq.edu.au](mailto:Sourish.Banerjee@unisq.edu.au) (S. Banerjee), [Allan.Manalo@unisq.edu.au](mailto:Allan.Manalo@unisq.edu.au) (A. Manalo).

<https://doi.org/10.1016/j.cscm.2024.e02891>

Received 1 October 2023; Received in revised form 8 December 2023; Accepted 15 January 2024

Available online 17 January 2024

2214-5095/© 2024 The Author(s). Published by Elsevier Ltd. This is an open access article under the CC BY license (<http://creativecommons.org/licenses/by/4.0/>).

### Nomenclature

$t_o$	thickness of the outer panel.
$t_i$	thickness of the inner panel.
$t_m$	thickness of the cement grout (i.e., matrix).
$H$	depth of the outer panel.
$h$	depth of the inner panel.
$A_o$	cross-sectional area of the outer GFRP profile.
$A_i$	cross-sectional area of the inner GFRP profile.
$L_1$	top unbonded length of inner panel.
$L_2$	length of overlap segment.
$\Delta L_1$	reduction of length $L_1$ due to compression load.
$\Delta L_2$	reduction of length $L_2$ due to compression load.
$\Delta s_m$	shear deformation of the cement grout.
$\Delta$	total displacement of the specimen.
$P$	applied load.
$E_o$	compression modulus of elasticity of outer GFRP profile.
$E_i$	compression modulus of elasticity of inner GFRP profile.
$G_m$	shear modulus of elasticity of cement grout.

very expensive material. Therefore, a low-cost binder is needed in order to make railway sleepers cost competitive. A cement grout is one such binder. Fig. 1 illustrates how cement grout is conceptualised to create a bond between the waste-based filler and the pultruded GFRP profiles of the composite railway sleeper.

In concrete structures, the use of pultruded GFRP profiles poses a number of challenges. Due to the smoothness of the profile surfaces, the profiles do not bond well to the concrete [12]. Several studies [13–16] have investigated the mechanical properties of beams and columns using pultruded FRP profiles as external reinforcement elements to improve compressive, flexural, and shear capacities. According to these studies, the interfacial bond between the FRP and concrete plays a critical role in the reinforcement effectiveness of FRP-concrete beams, as the stress transfers from the concrete to the FRP component at this interface and vice versa. In order to overcome this challenge, the surface roughness of the profile needs to be improved. Lu et al. [17] studied the bond performance of sand coated GFRP bars in high-performance concrete. In this study, it was concluded that the coating of sand on reinforcing bars could increase the bond strength between concrete and reinforcing bars. Yuan et al. [18] studied the GFRP pultruded I-section coated with sand to investigate the influence of sand coating on bond behaviour when embedded in concrete. The findings of this study indicate that sand coatings improve the bond strength significantly. In another study, Yuan et al. [19] examined the bond strength between GFRP pultruded profiles and concrete using self-compacting concrete and normal concrete. In this study, it was found that the type of concrete material can have an impact on bond performance.

Predicting the bond behaviour of composite materials is an engineering challenge. There are a number of factors that influence bonding performance, such as surface treatment and matrix behaviour. Developing comprehensive models that can capture these multifaceted interactions remains a challenging task due to the need for extensive experimental data and sophisticated computational techniques. While researchers have attempted to predict the bond behaviour using complex computer simulations [20] or artificial neural networks [21], a simple theoretical model has always attracted the attention of researchers.

While the studies cited above highlighted the challenges associated with bonding FRP to concrete, they did not describe how to overcome these challenges. Based on the findings in the literature, this study identified four potential methods for improving bond strength between GFRP profiles and low-cost cement grout. These methods consist of a) adding angular sand in different proportions to

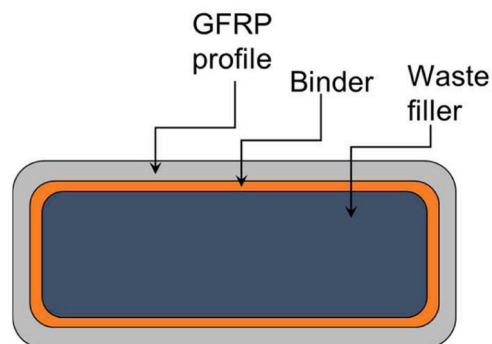


Fig. 1. Concept of cement grout as a binder between GFRP profile and waste filler for railway sleeper.

cement grout, b) adding different sizes of angular sand to cement grout, c) increasing the roughness of the bond surface of GFRP profiles, and d) using different types of cements in grout preparation. To test this hypothesis, a comprehensive experimental study was conducted. In order to predict the bond strength within the scope of this study, a suitable theoretical model was developed. In general, the outcome of this study will be beneficial to civil engineers when designing reinforced concrete structures using pultruded GFRP profiles.

## 2. Experimental program

### 2.1. Materials

#### 2.1.1. Glass sand

Recycled glass waste is used to make glass sand made from 100 % recycled glass. The waste glass is screened, crushed into smaller pieces, and washed methodically before being graded into a product similar to natural sand. Three sizes of glass sand (coarse, medium, and fine) were used in this study. The reason for using three sizes of sand is the variation in surface area which determines the bonding characteristics. Unlike sea sand, these glass sands have an angular shape, which ensures greater bonding due to their rough surface. Enviro Sand, a supplier based in Australia, has provided this glass sand. Table 1 provides the particle size and density of three different types of glass sand.

#### 2.1.2. Cement

This study used three types of cement (shrinkage compensating cement, expanding cement, general purpose cement). Three types of cement are used due to their unique bonding characteristics. As the name suggests, shrinkage compensating cement is a mixture of Portland cement, carefully selected and graded aggregates, and admixtures that can be used to compensate for shrinkage in cementitious grouts. A similar appearance to concrete is achieved with this product, which contains no chlorides or corrosion-causing agents. In contrast, expanding cement balances drying shrinkage, causing it to tightly grip embedded items and surrounding materials. This type of cement, which is more expensive than traditional cements, was chosen because of its expansion characteristics. General purpose cement, however, is a highly reliable, economical, and high-quality building material. Due to its versatility and consistency, GP cement is ideal for virtually all construction applications. The densities of these cements are listed in Table 1.

#### 2.1.3. GFRP hollow tubes

The GFRP square hollow sections that Wagners Pty Ltd. supplied were made using the pultrusion process. This structural profile is made from vinyl ester resin and glass fibre reinforcements. Two different sizes of pultruded profiles were used in this study. Nominal dimensions of the section were 125 mm (depth) × 125 mm (width) × 6.40 mm (thick) and 100 mm (depth) × 100 mm (width) × 5.20 mm (thick), with a gross sectional area of 2970 mm<sup>2</sup> and 1905 mm<sup>2</sup> and mass of 6.07 kg/m and 3.85 kg/m, respectively. The properties were determined according to the technical data sheet provided by the manufacturer (Wagners Pty Ltd [22]). In addition to being lightweight, highly durable, and virtually maintenance-free, fibreglass tubes offer a variety of advantages. This type of profile is currently used in a number of structural applications, including piles, crossarms for power poles, decking, handrails, boardwalks, and many other applications.

### 2.2. Methods

#### 2.2.1. Design of experiments

This study aims at understanding the impact of different influential parameters on the bond behaviour of GFRP tubes in order to determine the effectiveness of various bonding methods. The bond performance may be affected by several factors, including grout properties, grout materials, and the surface characteristics of the GFRP tube. This study examines the volume (0–20 % by volume) and size of sands (fine to coarse) in grout, GFRP surface treatment (no treatment, pre-coating and sanding) and different cementitious materials (shrinkage compensating, expanding cement and GP cement) to understand the effect of such critical parameters. The range of these parameters were selected to create surface roughness without significantly affecting the bonding properties of the grout. Experiments were designed to minimise specimen numbers while still investigating the effect of critical parameters. A total of 9 cases were studied, each with three samples. A detailed description of these 9 cases can be found in Table 2. Cases number 1 to 3 represent the effect of the different percentages of glass volume in the grout mix, whereas case numbers 3 to 5 represent the effect of glass sizes,

**Table 1**  
Properties of glass sand and cement (Provided by the supplier of the material).

Materials	Particle size	Density (g/cm <sup>3</sup> )
Coarse glass sand	1.7–3.35 mm	2.18
Medium glass sand	1.0–1.7 mm	2.10
Fine glass sand	0.5–1.0 mm	2.00
Shrinkage compensating cement	3–30 μm	1.87
Expanding cement	3–30 μm	1.48
General purpose cement	3–30 μm	1.54

case numbers 5 to 7 demonstrate the effect of surface treatment on GFRP tubes and cases 5, 8 and 9 demonstrate the effect of binder type. To investigate the effect of each parameter, this study ensures that the other design parameters are to remain the same within each study group.

### 2.2.2. Sample preparation and testing

The specimen was prepared by inserting a smaller tube (100 mm × 100 mm) into a larger tube (125 mm × 125 mm) and filling the small gap between the tubes with cementitious grout. To facilitate casting and testing, the external tube (125 mm × 125 mm) was cut by 100 mm and the internal tube (100 mm × 100 mm) by 125 mm. The bottoms of the tubes were level and sealed with plastic wrap to prevent the grout from flowing off. Some specimens were then pre-coated (Case 6) and sanded (Case 7) on their external and internal surfaces. Polyester resin and glass sands were used to precoat the bonded surfaces of both profiles, i.e., the internal surfaces of the larger profile and the external surfaces of the smaller profile. Pre-coated GFRP profiles were kept at room temperature for 24 h to dry. Similarly, sanding was performed on the bonding surfaces using sandpaper. All other samples were prepared without any surface treatment. Fig. 2(a) shows that 27 specimens (i.e., 9 cases with three samples each) were prepared for bond testing.

MTS equipment capable of handling 100 kN of compression load was used for the testing. In order to allow movement of the interior profile under applied load, a 25 mm long GFRP profile with the same cross-sectional dimensions as the external profile was placed at the bottom of the specimen (Fig. 2b). All the specimens failed in shear, and a representation of the failure mode is presented in Fig. 2(c). Testing of all the samples was conducted in the same way where the load on the panel was gradually increased until the bond failed.

## 3. Results and discussion

The results of specimens 1, 2 and 3 with a total of 9 cases are outlined in Table 3. The effect of glass sand volume, glass size, surface treatment and binder types were critically analysed and discussed in the following sections. The bond strength in Table 3 was calculated based on the failure load divided by the bond surface area. The standard deviation of the bond properties is affected by the complex shear behaviour of the non-homogenous binding materials.

### 3.1. Effect of glass sands

The effect of the percentage of glass sand volume is shown in Fig. 3. Load-displacement behaviour was slightly nonlinear at the beginning of the experiment, but linear behaviour was observed in the second half. Perhaps this is due to the initial settlement of the specimens. After the specimen was settled and compacted, a linear load-displacement relationship was observed (Fig. 3a). In general, the percentage of glass sand volume in binding material has only a small impact on the average bond strength (Fig. 3b). A difference of less than 5 kPa in average bond strength was observed when the percentage of glass sand in cement grout increased from 0 to 20 %. Based on the results, this small variation may be due to the fact that the cementitious grout was used only to cover the bond surface of the GFRP profiles, while the sand did not increase the roughness of the surface.

### 3.2. Effect of glass sand size

The bond strength of three different sizes of glass sand in binding materials can be seen in Fig. 4. Glass sand of fine or medium size offers similar bond strength, while glass sand of coarse size offers lower bond strength. In Fig. 4(a), there was a similar nature of load-displacement behaviour to that observed in Fig. 3(a), where a linear increase in load-displacement behaviour was seen after the initial settlement. The average bond strength for the fine and medium sands was 159 kPa and 171 kPa, respectively, while the coarse sand provided only 128 kPa. Perhaps the decrease in bond strength with coarse sand may be attributed to the fact that the bond surface area of the GFRP profile was partially covered by the larger particles of glass sand. This resulted in a reduction in the effective bonding surface area for cement grout, which is primarily responsible for creating the bond strength.

**Table 2**  
Design of experiments.

Case number	Sample number	glass content	glass size	surface treatment	Binder types	Remarks
1	1–3	0 %	Medium	No treatment	Shrinkage compensating	Effect of glass sand content
2	4–6	10 % by vol	Medium	No treatment	Shrinkage compensating	Case 1–Case 3
3	7–9	20 % by vol	Medium	No treatment	Shrinkage compensating	
4	10–12	20 % by vol	Coarse	No treatment	Shrinkage compensating	Effect of glass size
5	13–15	20 % by vol	Fine	No treatment	Shrinkage compensating	Case 3–Case 5
6	16–18	20 % by vol	Fine	Pre-coating	Shrinkage compensating	Effect of surface treatment
7	19–21	20 % by vol	Fine	Sanding	Shrinkage compensating	Case 5–Case 7
8	22–24	20 % by vol	Fine	No treatment	Expanding Cement	Effect of binder types
9	25–27	20 % by vol	Fine	No treatment	GP cement	Case 5, 8 and 9

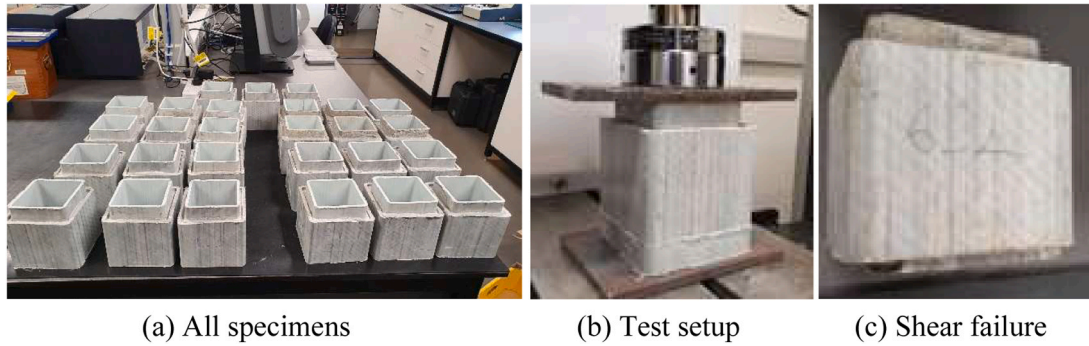


Fig. 2. Specimens, test set-up and failure mode.

Table 3  
Test results of all specimens.

Bond strength (kPa)	Case 1	Case 2	Case 3	Case 4	Case 5	Case 6	Case 7	Case 8	Case 9
Specimen 1	201	223	83	130	149	536	261	173	133
Specimen 2	200	145	202	131	150	716	201	101	190
Specimen 3	113	155	229	123	177	572	238	137	156
Average	171	174	171	128	159	608	233	137	160
Standard dev.	50.44	42.49	77.61	4.17	16.23	95.33	30.27	36.18	28.71

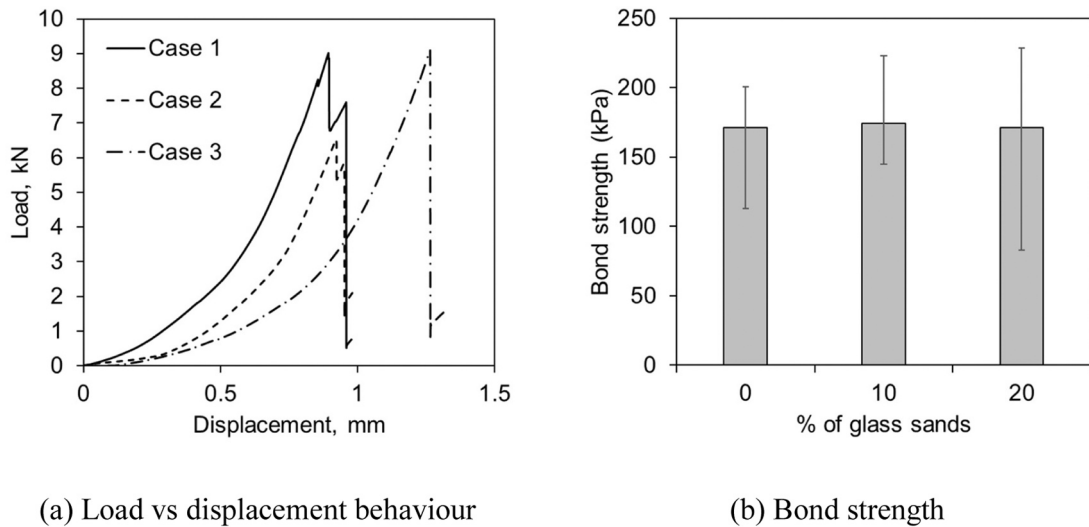


Fig. 3. Variation of bond strength with the increase of sand content.

3.3. Effect of surface treatment

In order to evaluate the effect of surface treatment, it is necessary to analyse the behaviour of specimens for Case 5, Case 6 and Case 7 since the surfaces of the GFRP profile in these three specimens were treated differently. In Case 5, the surface of the GFRP profile was left as it was (i.e., no treatment) while in Case 6, a resin and glass sand mixture was applied to the surface of the GFRP profiles (i.e., pre-coating). Before preparing the specimens for Case 7, a rough bond surface was created on the GFRP profile by sanding. There was a significant variation in bond strength as a result of the variation in surface treatment. There was a bond strength of 159 kPa, 608 kPa, and 233 kPa for specimens without treatment, pre-coating, and sanding, respectively (Fig. 5). The pre-coating of the bond surface increased the bond strength by 3.8 times compared with the bond surface that was not treated. On the other hand, the sanding of the bond surface increased the bond strength by 1.5 times compared to no surface treatment. It is therefore implied that pre-coating creates a highly rough bond surface, which enhances bond strength. The sanding method also produced a rough surface, but its roughness was not as high as that produced by the pre-coating method.

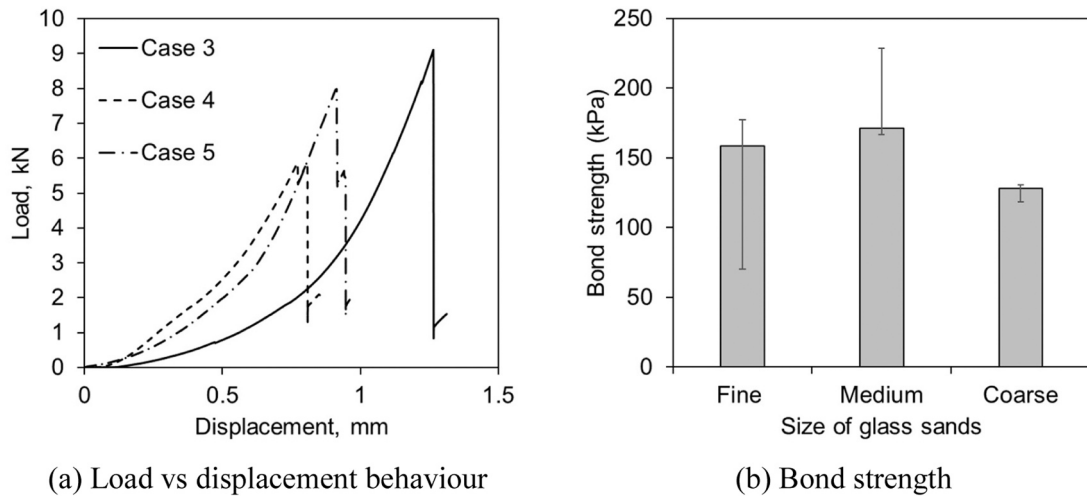


Fig. 4. Variation of bond strength with the increase of sand size.

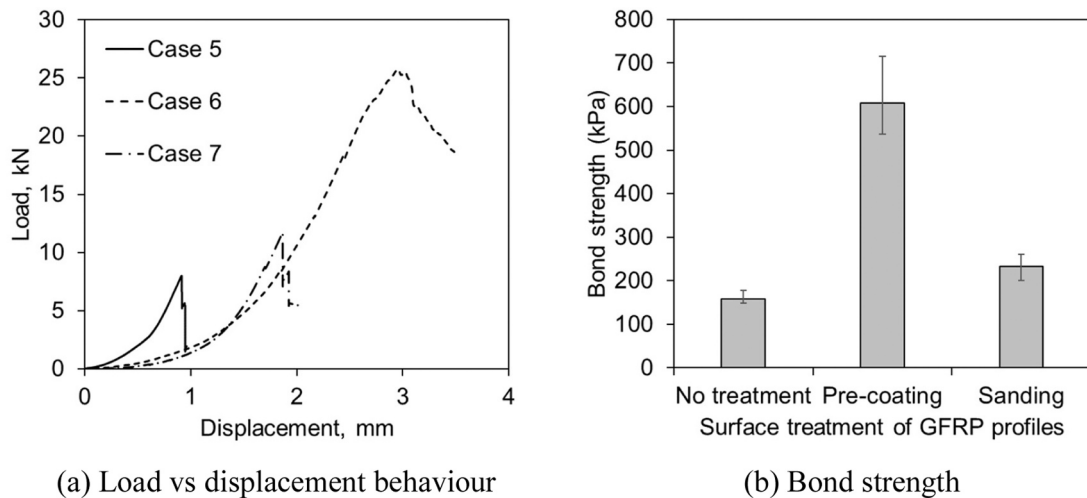
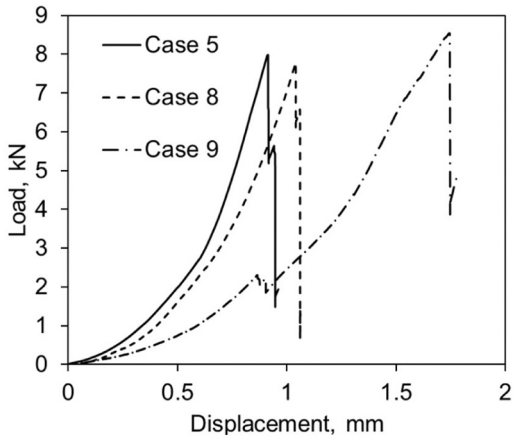


Fig. 5. Variation of bond strength with surface treatment of GFRP profiles.

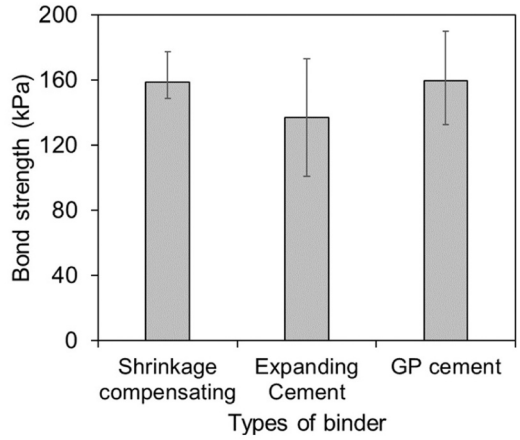
### 3.4. Effect of binder types

The effect of the binder type can be studied by analysing the results of Case 5, Case 8 and Case 9 where shrinkage compensating, expanding cement and GP cement were used in the binder, respectively. The shrinkage compensating cement aims to offset the contraction of binder due to drying shrinkage by expanding the volume during the hardening process. Expanding cement generally expands the binder when hardened. GP cement, however, does not exhibit this type of binder movement. A purpose of introducing different types of cement is to understand how cement expansion characteristics influence bond strength. The results indicated that the average bond strengths of the binder with shrinkage compensating cement, expanding cement and GP cement were 159 kPa, 137 kPa, and 160 kPa, respectively (Fig. 6). Surprisingly, expanding cement binder provided the lowest bond strength compared to the other two cement binders. This is an interesting finding as it was expected that the expansion characteristics of expanding cement would improve the bond strength. It is possible that the lower bond strength of expanding cement binder is due to the movement of matrix as a result of the gradual expansion, which weakens the bond between the GFRP profile and the cement binder. Shrinkage compensating cement and GP cement binder did not move as much as expanding cement binder, which creates a stronger bond with the surface of GFRP profiles.

This study found that the volume of glass sand, the size of glass sand, the surface treatment of GFRP profiles, and the type of binder can affect the bond strength by 2 %, 34 %, 282 %, and 17 %, respectively. The results indicate that surface treatment is the most effective method for improving bond strength followed by variation of glass sand size, different types of binder, and adding glass sand to grout.

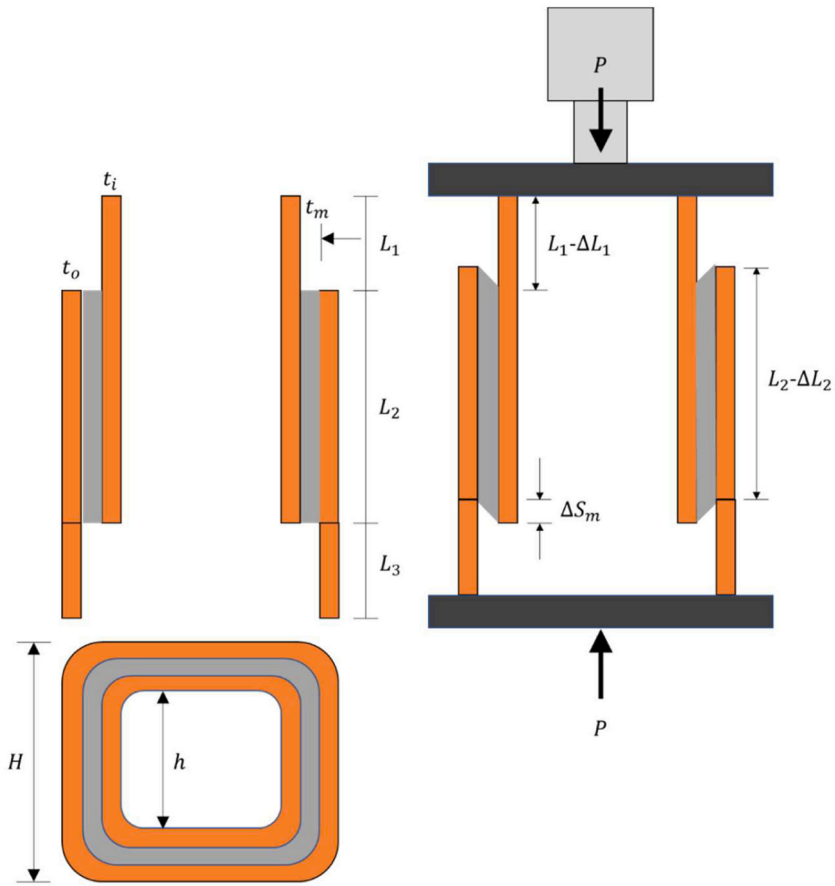


(a) Load vs displacement behaviour



(b) Bond strength

Fig. 6. Variation of bond strength with the types of binder.



(a) original shape

(b) deflected shape

Fig. 7. Schematic diagram of the specimen for analytical solution.



## 4. Theoretical modelling

### 4.1. Model development

A theoretical model has been developed to predict bond strength. Model parameters include the dimensions and surface roughness of GFRP profiles, as well as the properties of GFRP profiles and cement binder. A schematic diagram of the section of specimen is shown in Fig. 7. In order to develop the model, linear elastic properties of materials were taken into consideration. This can be justified by the linear elastic load-displacement behaviour of the specimens after initial settlement under loads (Fig. 3 to Fig. 6).

From Fig. 1,

$$A_i E_i = 4t_i(h + t_i)E_i \quad (1)$$

$$A_o E_o = 4t_o(H - t_o)E_o \quad (2)$$

The properties of the GFRP material were obtained from the supplier's technical data sheet [22].

**(a) Deflection in unbonded segment (length  $L_1$  and  $L_3$ ).**

In unbonded segment,  $P$  load is acting on the cross-section  $A_i$ , and therefore,

$$\text{Compressive stress, } \sigma_1 = \frac{P}{A_i} \quad (3)$$

$$\text{Compressive strain, } \varepsilon_1 = \frac{\sigma_1}{E_i} = \frac{P}{A_i E_i} \quad (4)$$

The axial displacement of the inner-panel segment can be derived as

$$\Delta L_1 = \varepsilon_1 \times L_1 \quad (5)$$

Using Eqs. (1), (4) and (5).

$$\Delta L_1 = \frac{PL_1}{4t_i(h + t_i)E_i} \quad (6)$$

Similarly,

$$\Delta L_3 = \frac{PL_3}{4t_o(H - t_o)E_o} \quad (7)$$

**(b) Deflection in overlap segment (length  $L_2$ ).**

The total deflection of the overlap segment is the sum of the axial deflection in outer-panel and the shear deflection in the cement grout.

In this segment, half of the reaction force  $P$  is transferred in the outer panel and the axial deformation is calculated as

$$\Delta L_2 = \frac{PL_2}{4t_o(H - t_o)E_o f_r} \quad (8)$$

In Eq. (8),  $f_r$  represents roughness factor of the GFRP profile. Since the surface of the GFRP profiles was very smooth, it was assumed the roughness factor to be very similar to general steel pipes (i.e.,  $f_r = 0.015$  [23]). However, the roughness factors were increased to 0.020 and 0.018 when the GFRP profiles were pre-coated and sanded, respectively.

In the linear elastic range, the axial displacement of the cement grout due to the shear deformation would be the same whether it is calculated from an exact stress distribution or from the average shear stress of the matrix.

$$\text{Average shear stress, } \tau_{ave} = \frac{P}{(H - 2t_o - t_m)t_m f_r} \quad (9)$$

$$\text{Shear strain, } \gamma = \frac{\tau_{ave}}{G_m} \quad (10)$$

The axial displacement due to shear deformation of cement grout is

$$\Delta s_m = t_m \gamma \quad (11)$$

Using Eqs. (9), (10) and (11).

$$\Delta s_m = \frac{P}{(H - 2t_o - t_m)G_m f_r} \quad (12)$$

**(c) Global axial displacement.**

The global axial displacement is the sum of all displacement.

$$\Delta = \Delta L_1 + \Delta L_2 + \Delta L_3 + \Delta s_m$$



$$\Delta = \frac{PL_1}{4t_i(h+t_i)E_i} + \frac{PL_2}{4t_o(H-t_o)E_{ofr}} + \frac{PL_3}{4t_o(H-t_o)E_o} + \frac{P}{(H-2t_o-t_m)G_m f_r}$$

$$P = \frac{\Delta}{\left[ \frac{L_1}{4t_i(h+t_i)E_i} + \frac{L_2}{4t_o(H-t_o)E_{ofr}} + \frac{L_3}{4t_o(H-t_o)E_o} + \frac{1}{(H-2t_o-t_m)G_m f_r} \right]} \quad (13)$$

Eq. (13) represents the theoretical load.

#### 4.2. Model validation

The theoretical load can be calculated by using Eq. (13) when the deflection is known. The experimental deflection was taken into account in Eq. (13) in order to verify the model. A comparison was made between the load calculated from Eq. (13) and the experimental failure load shown in Table 4. It can be seen that the linear elastic models are reasonably able to predict the bond behaviour of the specimen.

Composites behave very differently from isotropic materials due to their unpredictable nature. As a result, the standard deviation of composite materials is expected to be higher than that of isotropic materials. It was found that the theoretical prediction was close to the average values of the experimental results. This theoretical model has the main contribution of allowing the bond behaviour of full composite panels to be predicted for a wide variety of composite panels bonded with a variety of cement grouts when their properties are known.

### 5. Conclusion

This study investigated the bond behaviour of cement matrix with GFRP profiles. Four different methods were studied to improve the bond behaviour. The effect of adding different percentages of glass sand in cement grout, the size of glass sand, surface treatment of GFRP profiles and the types of cement to prepare binder were investigated. A theoretical model was also developed to predict the bond behaviour. The findings of this study are provided below:

- The addition of glass sand up to 20 % does not appear to have a significant impact on the overall bonding behaviour (only 2 % variation). GFRP profiles are bonded primarily by cement paste and glass sand cannot increase surface roughness when added to the binder.
- The size of the glass sand can have a significant impact on the bond strength (up to 34 % variation). Based on the results of this study, an increase in the size of sand particles reduces the bond strength as a result of the reduction of the effective bond surface area due to the presence of sand particles. The larger the sand particles, the smaller the effective bond area.
- This study found that increasing surface roughness on the bonded area is the most effective method of improving bond strength (up to 282 % variation). A pre-coating of the bond surface with resin and glass sand mix creates a highly rough surface which increases bond strength by 3.8 times when compared to an untreated bond surface. In contrast, sanding the bond surface is not as effective as pre-coating, but it can increase bond strength by 1.5 times over untreated surfaces.
- Bond strength is affected by the characteristics of the cement binder (up to 17 % variation). The expansion and contraction characteristics of cement make it less effective for bonding. Internal movement of binder caused by the expansion and contraction of binder volume during the hardening process can weaken the bond strength.
- A linear elastic model can be used to predict the bond behaviour. The properties of the GFRP profile and cement binder are the key parameters that affect bond behaviour. It is, however, necessary to take into account the bond surface roughness coefficient when predicting the bond strength.

The results of this study have provided new insight into how to improve the bond behaviour between smooth surfaces of GFRP profiles and a low-cost binder. For an economic solution, it is important to determine the benefit-cost ratio of different methods. The findings of this study will be of value to design engineers and end users seeking to bond GFRP profiles to low-cost materials in end use

**Table 4**  
Variation between experimental and theoretical failure load.

Case No.	Experimental P (kN)	Theoretical P (kN)
1	7.71 ± 2.3	5.59
2	7.84 ± 1.9	6.69
3	7.72 ± 3.5	9.36
4	5.77 ± 0.2	6.04
5	7.14 ± 0.7	6.12
6	27.36 ± 4.3	26.55
7	10.49 ± 1.4	14.69
8	6.17 ± 1.6	7.10
9	7.18 ± 1.3	11.38

applications.

### CRedit authorship contribution statement

**Mamun Abdullah:** Conceptualization, Data curation, Formal analysis, Investigation, Methodology, Validation, Writing – original draft. **Ferdous Wahid:** Conceptualization, Methodology, Supervision, Writing – review & editing. **Banerjee Sourish:** Supervision, Writing – review & editing. **Manalo Allan:** Supervision, Writing – review & editing.

### Declaration of Competing Interest

The authors declare that they have no known competing financial interests or personal relationships that could have appeared to influence the work reported in this paper.

### Data Availability

Data will be made available on request.

### Acknowledgements

The authors would like to acknowledge Enviro Sand Pty Ltd and Wagners Pty Ltd for their generous in-kind contributions to supply materials. The first and second authors would like to acknowledge the financial support they received from the Advance Queensland Industry Research Fellowship (AQIRF 098-2021RD4) program.

### References

- [1] T. Liu, X. Liu, P. Feng, A comprehensive review on mechanical properties of pultruded FRP composites subjected to long-term environmental effects, *Compos. Part B: Eng.* 191 (2020) 107958.
- [2] A.K. Gand, T.-M. Chan, J.T. Mottram, Civil and structural engineering applications, recent trends, research and developments on pultruded fiber reinforced polymer closed sections: a review, *Front. Struct. Civ. Eng.* 7 (2013) 227–244.
- [3] C.E. Bakis, et al., Fiber-reinforced polymer composites for construction—state-of-the-art review, *J. Compos. Constr.* 6 (2) (2002) 73–87.
- [4] J.R. Correia, Y. Bai, T. Keller, A review of the fire behaviour of pultruded GFRP structural profiles for civil engineering applications, *Compos. Struct.* 127 (2015) 267–287.
- [5] X. Zou, H. Lin, P. Feng, Y. Bao, J. Wang, A review on FRP-concrete hybrid sections for bridge applications, *Compos. Struct.* 262 (2021) 113336.
- [6] Y.M. Amran, R. Alyousef, R.S. Rashid, H. Alabduljabbar, C.-C. Hung, Properties and applications of FRP in strengthening RC structures: a review, *Structures* 16 (2018) 208–238 (Elsevier).
- [7] A. Sharda, et al., Axial compression behaviour of all-composite modular wall system, *Compos. Struct.* 268 (2021) 113986.
- [8] W. Ferdous, A.D. Almutairi, Y. Huang, Y. Bai, Short-term flexural behaviour of concrete filled pultruded GFRP cellular and tubular sections with pin-eye connections for modular retaining wall construction, *Compos. Struct.* 206 (2018) 1–10.
- [9] E. Guades, T. Aravinthan, M. Islam, A. Manalo, A review on the driving performance of FRP composite piles, *Compos. Struct.* 94 (6) (2012) 1932–1942.
- [10] A.A. Mohammed, et al., Effectiveness of a novel composite jacket in repairing damaged reinforced concrete structures subject to flexural loads, *Compos. Struct.* 233 (2020) 111634.
- [11] W. Ferdous, et al., Static behaviour of glass fibre reinforced novel composite sleepers for mainline railway track, *Eng. Struct.* vol. 229 (2021) 111627.
- [12] A.M. Ali, L. Dieng, R. Masmoudi, "Experimental, analytical and numerical assessment of the bond-slip behaviour in concrete-filled-FRP tubes," *Eng. Struct.* vol. 225 (2020) 111254.
- [13] Z. Guo, X. Xue, M. Ye, Y. Chen, Z. Li, Experimental research on pultruded concrete-filled GFRP tubular short columns externally strengthened with CFRP, *Compos. Struct.* 255 (2021) 112943.
- [14] Y. Qasrawi, P.J. Heffernan, A. Fam, Performance of concrete-filled FRP tubes under field close-in blast loading, *J. Compos. Constr.* 19 (4) (2015) 04014067.
- [15] T. Vincent, T. Ozbakkaloglu, Influence of fiber orientation and specimen end condition on axial compressive behavior of FRP-confined concrete, *Constr. Build. Mater.* 47 (2013) 814–826.
- [16] T. Ozbakkaloglu, T. Xie, Geopolymer concrete-filled FRP tubes: behavior of circular and square columns under axial compression, *Compos. Part B: Eng.* 96 (2016) 215–230.
- [17] J. Lu, H.M. Afefy, H. Azimi, K. Sennah, M. Sayed-Ahmed, Bond performance of sand-coated and ribbed-surface glass fiber reinforced polymer bars in high-performance concrete, *Structures* 34 (2021) 10–19 (Elsevier).
- [18] J.S. Yuan, M.N. Hadi, Bond-slip behaviour between GFRP I-section and concrete, *Compos. Part B: Eng.* 130 (2017) 76–89.
- [19] J.S. Yuan, M.N. Hadi, Friction coefficient between FRP pultruded profiles and concrete, *Mater. Struct.* 51 (5) (2018) 120.
- [20] H. Yin, K. Shirai, W. Teo, Numerical model for predicting the structural response of composite UHPC–concrete members considering the bond strength at the interface, *Compos. Struct.* 215 (2019) 185–197.
- [21] A. Cascardi, F. Micelli, ANN-based model for the prediction of the bond strength between FRP and concrete, *Fibers* 9 (7) (2021) 46.
- [22] Wagners, "Composite Fibre Technologies - Product guide," Wagners CFT Manufacturing Pty Ltd, 2021, vol. 5.
- [23] Engineering-tools. "Surface roughness of common materials (myengineeringtools.com)." (accessed 22/07/2023).